ELECTROMAGNETIC MODELING AND EXPERIMENTAL VERIFICATION OF A COMPLETE WAVEGUIDE-BASED APERTURE-COUPLED PATCH AMPLIFIER ARRAY

Alexander B. Yakovlev[1], Sean Ortiz[1], Mete Ozkar[1], Amir Mortazawi[1], and Michael B. Steer[2]

[1]Department of Electrical and Computer Engineering, North Carolina State University, Raleigh, NC 27695-7914, USA
[2]Institute of Microwaves and Photonics, School of Electronic and Electrical Engineering, The University of Leeds, Leeds, LS2 9JT, United Kingdom

Abstract— **In this paper, electromagnetic modeling and experimental validation of a waveguide-based spatial power combining array are presented. Here, an aperture-coupled patch array power combining system is modeled in its entirety. This includes a Method of Moments (MoM) integral equation formulation of the Generalized Scattering Matrix (GSM) for a N-port patch-slot-waveguide transition and the mode-matching analysis of the GSM for the receiving and transmitting rectangular waveguide tapers. An overall response of the system is obtained by cascading GSMs of electromagnetic structures and the S-parameters of amplifier networks. Numerical and experimental results are shown for the single unit cell, 2×3 and 3×4 amplifier arrays operating at X-band.**

I. INTRODUCTION

The demand for high-power and efficient microwave and millimeter-wave amplifiers has created a large amount of theoretical and experimental research in the area of open [1]– [4] and waveguide-based [5]– [9] spatial and quasi-optical power combining systems. Due to the complexity of these structures there is a great need for the electromagnetic modeling and analysis of spatial power combining systems, including a better understanding of important issues such as multimoding effects, surface waves, and device/field interactions. For the accurate analysis of open and waveguide-based power combining systems, it is necessary to model the entire system, including a full-wave analysis of passive structures and the interaction of passive elements and active devices.

In this paper, we present results of electromagnetic modeling and measurements of a waveguide-based aperture-coupled patch amplifier array shown in Fig. 1. The amplifier array has been recently designed, fabricated, and tested with hard horn excitation [10]. The incident signal from the feed horn couples into an array of patch antennas. Each antenna is coupled to a microstrip line through a slot-coupled single-mode waveguide transition [11]. Each microstrip line feeds an amplifier network. The output signal is then coupled to an output horn via the same waveguide transition described above.

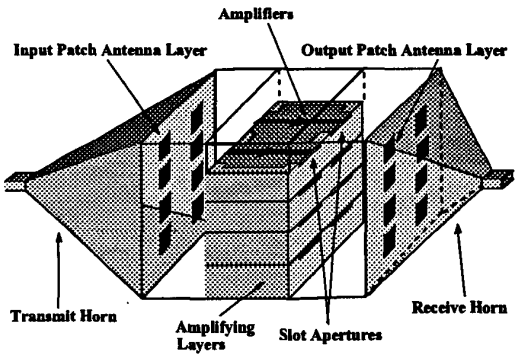

Fig. 1. A waveguide-based aperture-coupled patch amplifier array.

A full-wave integral equation formulation is developed for the electromagnetic modeling of a waveguide to aperture-coupled patch array, resulting in the GSM of a N-port device. A coupled set of the electric field and magnetic field integral equations (with dyadic Green's functions obtained for layered waveguides) is discretized via the MoM for the electric and magnetic current density. This provides an accurate model of the patch-to-slot coupling at each port for all propagating and evanescent TE and TM modes. The GSM for a rectangular waveguide taper is obtained using the mode-matching technique, where a linear taper is approximated by double-plane stepped junctions similar to [12]. All mod-

0-7803-5687-X/00/$10.00 © 2000 IEEE

ules within the power combining system including the amplifier network are cascaded to get an overall response (return loss and gain). The structure was simulated and tested for a single unit cell and a 2×3 and 3×4 element amplifier array.

II. Full-Wave System Modeling

An electromagnetic modeling of the entire spatial power combining amplifier (Fig. 1) is based on the decomposition of the system into modules, including rectangular waveguide tapers (feeding/collecting), N-port aperture-coupled patch array waveguide transitions, waveguide-microstrip line junctions, and amplifier circuits. Each of these modules has to be rigorously analyzed in order to obtain an accurate response of the entire system.

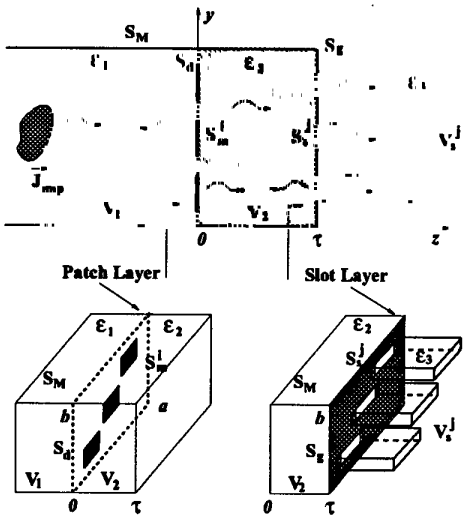

Fig. 2. Geometry of N-port aperture-coupled patch array waveguide transition.

Consider the N-port patch array to waveguide transition shown in Fig. 2. Rectangular patch antennas S_m^i and slot apertures S_s^j in a ground plane S_g are located on the opposite interfaces of dielectric layer with permittivity ϵ_2. Note that each of the slot-coupled waveguides (regions V_s^j) is filled with the same dielectric material (ϵ_3). The incident electric and magnetic fields in the large waveguide (region V_1) are generated by an impressed electric current source $\overline{\mathbf{J}}_{imp}$ ($\nabla \times \overline{\mathbf{J}}_{imp}$ for the magnetic field). It should be noted that an incident magnetic field from each of the waveguides V_s^j is similarly handled.

A coupled set of integral equations is obtained by enforcing the boundary condition on the tangential components of the electric field on the conductive surfaces S_m^i at $z = 0$ and the continuity condition on the tangential components of the magnetic field on the magnetic surfaces (slot apertures) S_s^j at $z = \tau$ (similar formulations have been presented in [13]). The integral form of the electric-field boundary condition is obtained using the second vector-dyadic Green's theorem (with appropriate boundary and continuity conditions):

$$\hat{z} \times \overline{\mathbf{E}}_1^{inc}(\vec{r}) = j\omega\mu_0 \hat{z} \times \sum_{i=1}^{N_m} \int_{S_m^i} \overline{\mathbf{J}}_i(\vec{r}') \cdot \overline{\overline{\mathbf{G}}}_{e1}^{(11)}(\vec{r}', \vec{r}) dS' - \hat{z} \times \sum_{j=1}^{N_s} \int_{S_s^j} \overline{\mathbf{M}}_j(\vec{r}') \cdot [\nabla' \times \overline{\overline{\mathbf{G}}}_{e1}^{(21)}(\vec{r}', \vec{r})] dS' . \quad (1)$$

The electric dyadic Green's functions, $\overline{\overline{\mathbf{G}}}_{e1}^{(11)}(\vec{r}, \vec{r}')$ and, $\overline{\overline{\mathbf{G}}}_{e1}^{(21)}(\vec{r}, \vec{r}')$, are obtained as the solution of the boundary-value problem for a semi-infinite partially filled waveguide (regions V_1 and V_2) terminated by a ground plane at $z = \tau$. They satisfy boundary and continuity conditions for the electric field on the surfaces S_M, S_g, and on the interface S_d.

The continuity condition for the tangential components of the magnetic field at $z = \tau$ results in the magnetic-field integral equation:

$$\hat{z} \times \overline{\mathbf{H}}_2^{inc}(\vec{r}) = -\frac{\epsilon_2}{\epsilon_1} \hat{z} \times \sum_{i=1}^{N_m} \int_{S_m^i} \overline{\mathbf{J}}_i(\vec{r}') \cdot [\nabla' \times \overline{\overline{\mathbf{G}}}_{e2}^{(12)}(\vec{r}', \vec{r})] dS' - j\omega\epsilon_0 \hat{z} \times \sum_{j=1}^{N_s} \int_{S_s^j} \overline{\mathbf{M}}_j(\vec{r}') \cdot [\epsilon_2 \overline{\overline{\mathbf{G}}}_{e2}^{(22)}(\vec{r}', \vec{r}) + \epsilon_3 \overline{\overline{\mathbf{G}}}_{e2}^{(j)}(\vec{r}', \vec{r})] dS'. \quad (2)$$

The electric dyadic Green's functions $\overline{\overline{\mathbf{G}}}_{e2}^{(12)}(\vec{r}, \vec{r}')$, $\overline{\overline{\mathbf{G}}}_{e2}^{(22)}(\vec{r}, \vec{r}')$ have been derived for semi-infinite partially filled waveguide (regions V_1 and V_2) satisfying boundary and continuity conditions for the magnetic field vector. The electric dyadic Green's functions of the second kind $\overline{\overline{\mathbf{G}}}_{e2}^{(j)}(\vec{r}, \vec{r}')$ are obtained for the semi-infinite waveguides (regions V_s^j) terminated by a ground plane at $z = \tau$. Green's functions are obtained in terms of double series expansions over the complete system of eigenfunctions of the Helmholtz operator.

The incident electric $\overline{\mathbf{E}}_1^{inc}(\vec{r})$ and magnetic $\overline{\mathbf{H}}_2^{inc}(\vec{r})$ fields are expressed as a series eigenmode expansion for all propagating and evanescent TE

and TM modes. The MoM discretization for the electric and magnetic currents enables the reduction of a coupled set of functional equations (1) and (2) to a matrix system of algebraic equations with respect to the unknown coefficients in the currents expansion. The magnitudes of scattered (reflected and transmitted) modes are obtained in terms of current coefficients using a unity power normalization for the electric and magnetic vector functions. The GSM for the N-port waveguide transition is obtained by relating the magnitudes of incident and scattered modes at each port. It should be noted that in this formulation the GSM is constructed for the N coupled waveguides with all propagating and evanescent TE and TM modes at each waveguide. This is in order to cascade GSMs of the waveguide transition and transmitting and receiving rectangular waveguide tapers.

Rectangular waveguide tapers, approximated by double-plane stepped junctions, are analyzed using the mode-matching technique [12]. For each stepped junction, the GSM for propagating and evanescent TE and TM modes is obtained. The GSM of the linear taper is constructed by cascading GSMs of individual junctions. The accuracy of the algorithm depends on the number of modes and steps used to model the tapered waveguide.

The waveguide-microstrip line feed junction was designed using *HP HFSS*^{TM} with a center frequency of 10 GHz and a 10 dB return loss bandwidth of 400 MHz [10], [11]. The amplifier network presented in [10] was simulated using *HP ADS*^{TM}. Note that the S-parameters of *Mini-Circuits ERA1*^{TM} monolithic amplifiers were measured and incorporated in the modeling scheme to obtain a response of the entire amplifier network.

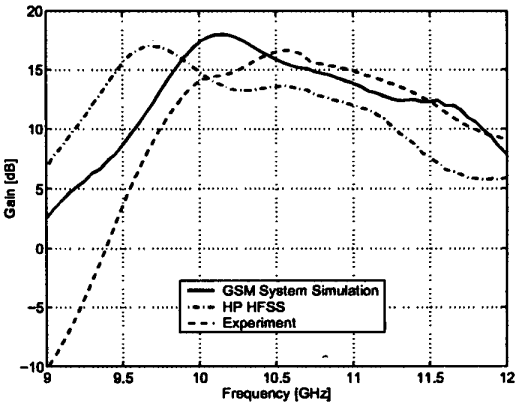

Fig. 3. Numerical and experimental results for the gain of the single aperture-coupled patch amplifier waveguide transition.

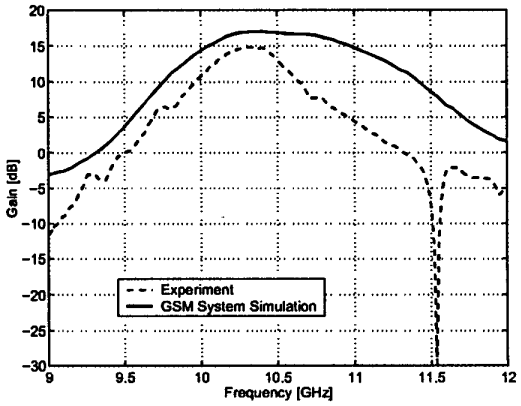

Fig. 4. Numerical and experimental results for the gain of the 2 × 3 waveguide-based aperture-coupled patch amplifier array.

III. Numerical and Experimental Results

In order to verify the accuracy of the full-wave modeling, three experiments were to be performed on a previously published amplifier array at X-band [10], [11]. The three experiments consist of the measurement of a unit cell, a 2 × 3 array, and finally a 3 × 4 array as shown in Fig. 1. Each unit cell of the three experiments contained an input aperture coupled patch antenna, a waveguide to microstrip transition, a two-stage amplifying circuit, a second microstrip to waveguide transition, and finally an output aperture coupled patch antenna. In the single unit cell measurement, a WR90 waveguide was used to feed the input and output antennas. The waveguide was placed in contact with the ground plane, and the dielectric of the patch antenna was fitted within the waveguide walls. The numerical model of the dielectric filled waveguide to patch antenna to WR90 waveguide was combined with measured data of the amplifier circuit and simulated microstrip to waveguide transitions. The results for the complete numerical model and experiment are shown in Fig. 3. The numerical model predicted the behavior of the circuit well and compares better with measured results than a commercial 3D Finite Element Method program.

The second experiment was performed in the same manner as the first experiment. For the 2 × 3 array, a 30.5 mm high, 46.0 mm wide, and 41.48 mm long horn was used to feed the array at both the input and output. The array was placed within the center of the horn so that the ground plane of the array was in contact with the aperture of the horn.

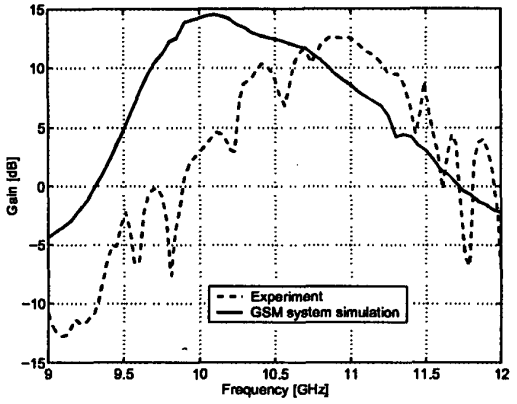

Fig. 5. Numerical and experimental results for the gain of the 3 × 4 waveguide-based aperture-coupled patch amplifier array.

The numerical and experimental results for the 2 × 3 array are shown in Fig. 4. For the 3 × 4 array experiment, a 53.975 mm high, 73.025 mm wide, and 107.33 mm long horn was used to feed the amplifier array. Full-wave simulation results of the system are shown in Fig. 5. The numerical model of the arrays presented accurately predicts the change in the resonant frequency caused by the cascading of the horn and waveguide to antenna GSMs. This behavior is not apparent when only considering the dominant mode coupling from the waveguide to aperture coupled patch array.

IV. Conclusion

Electromagnetic modeling and experimental verification are presented for the accurate analysis of a waveguide-based spatial power combining array. An aperture-coupled patch amplifier array is modeled in its entirety. This is accomplished by decomposing the system into electromagnetically-coupled modules, including rectangular waveguide tapers, aperture-coupled patch array to waveguide transitions, waveguide-microstrip line feed junctions, and amplifier networks. The overall response of the system is obtained by cascading GSMs of passive elements and the S-parameters of the amplifier networks. Numerical and experimental results are shown for a single unit cell and 2 × 3 and 3 × 4 amplifier arrays. This methodology can be effectively used for the electromagnetic modeling of various waveguide-based spatial and quasi-optical power combining systems leading to a better understanding of multimode and surface wave coupling effects and circuit/field interaction mechanisms.

V. Acknowledgments

This work is supported by an Army Research Office – MURI grant, under the Spatial and Quasi-Optical Power Combining DAAG-55-97-0132. Sean Ortiz is also supported by a NSF Graduate Fellowship.

References

[1] M. Kim, J. J. Rosenberg, R. P. Smith, R. M. Weikle, J. B. Hacker, M. P. Delisio, and D. B. Rutledge, "A grid amplifier," *IEEE Microwave Guided Wave Lett.*, vol. 11, Nov. 1991, pp. 322-324.

[2] M. Kim, E. A. Sovero, J. B. Hacker, M. P. Delisio, J.-C. Chiao, S.-J. Li, D. R. Gagnon, J. J. Rosenberg, and D. B. Rutledge, "A 100-element HBT grid amplifier," *IEEE Trans. Microwave Theory Tech.*, vol. 41, Oct. 1993, pp. 1762-1771.

[3] T. Ivanov, Ar. Balasubramaniyan, and A. Mortazawi, "One- and two-stage spatial amplifiers," *IEEE Trans. Microwave Theory Tech.*, vol. 43, Sept. 1995, pp. 2138-2143.

[4] M. N. Abdulla, U. A. Mughal, H.-S. Tsai, M. B. Steer, and R. A. York, "A full-wave system simulation of a folded-slot spatial power combining amplifier array," *IEEE Int. Microwave Symp. Dig.*, June 1999, pp. 559-562.

[5] A. Alexanian and R. A. York, "Broadband waveguide-based spatial combiners," *IEEE Int. Microwave Symp. Dig.*, June 1997, pp. 1139-1142.

[6] N.-S. Cheng, A. Alexanian, M. G. Case, and R. A. York, "20 watt spatial power combiner in waveguide," *IEEE Int. Microwave Symp. Dig.*, June 1998, pp. 1457-1460.

[7] N.-S. Cheng, A. Alexanian, M. G. Case, D. B. Rensch, and R. A. York, "40-W CW broad-band spatial power combiner using dense finline arrays," *IEEE Trans. Microwave Theory Tech.*, vol. 47, July 1999, pp. 1070-1076.

[8] N.-S. Cheng, T.-P. Dao, M. G. Case, D. B. Rensch, and R. A. York, "A 60-watt X-band spatially combined solid-state amplifier," *IEEE Int. Microwave Symp. Dig.*, June 1999, pp. 539-542.

[9] J. Hubert, L. Mirth, S. Ortiz, and A. Mortazawi, "A 4 watt Ka-band quasi-optical amplifier," *IEEE Int. Microwave Symp. Dig.*, June 1999, pp. 551-554.

[10] S. Ortiz and A. Mortazawi, "A perpendicularly-fed patch array for quasi-optical power combining," *IEEE Int. Microwave Symp. Dig.*, June 1999, pp. 667-670.

[11] S. Ortiz and A. Mortazawi, "A perpendicular aperture-fed patch antenna for quasi-optical amplifier arrays," *IEEE AP-S Int. Symp.*, July 1999, pp. 2386-2389.

[12] H. Patzelt and F. Arndt, "Double-plane steps in rectangular waveguides and their application for transformers, irises, and filters," *IEEE Trans. Microwave Theory Tech.*, vol. 30, May 1982, pp. 771-776.

[13] A. B. Yakovlev, A. I. Khalil, C. W. Hicks, A. Mortazawi, and M. B. Steer, "The generalized scattering matrix of closely spaced strip and slot layers in waveguide," *IEEE Trans. Microwave Theory Tech.*, vol. 48, Jan. 2000, pp. 126-137.